Dual-targeting immunotherapy of lymphoma: potent cytotoxicity of anti-CD20/CD74 bispecific antibodies in mantle cell and other lymphomas

Pankaj Gupta,[1] David M. Goldenberg,[2] Edmund A. Rossi,[3] Thomas M. Cardillo,[1] John C. Byrd,[4] Natarajan Muthusamy,[4] Richard R. Furman,[5] and Chien-Hsing Chang[1,3]

[1]Immunomedics Inc, Morris Plains, NJ; [2]Garden State Cancer Center, Center for Molecular Medicine and Immunology, Morris Plains, NJ; [3]IBC Pharmaceuticals, Morris Plains, NJ; [4]Division of Hematology, Department of Internal Medicine, College of Medicine, The Ohio State University, Columbus, OH; and [5]Weill-Cornell Medical College, New York, NY

We describe the use of novel bispecific hexavalent Abs (HexAbs) to enhance anticancer immunotherapy. Two bispecific HexAbs [IgG-$(Fab)_4$ constructed from veltuzumab (anti-CD20 IgG) and milatuzumab (anti-CD74 IgG)] show enhanced cytotoxicity in mantle cell lymphoma (MCL) and other lymphoma/leukemia cell lines, as well as patient tumor samples, without a crosslinking Ab, compared with their parental mAb counterparts, alone or in combination. The bispecific HexAbs have different properties from and are more potent than their parental mAbs in vitro. The juxtaposition of CD20 and CD74 on MCL cells by the HexAbs resulted in homotypic adhesion and triggered intracellular changes that include loss of mitochondrial transmembrane potential, production of reactive oxygen species, rapid and sustained phosphorylation of ERKs and JNK, down-regulation of pAkt and Bcl-xL, actin reorganization, and lysosomal membrane permeabilization, culminating in cell death. They also displayed different potencies in depleting lymphoma cells and normal B cells from whole blood ex vivo and significantly extended the survival of nude mice bearing MCL xenografts in a dose-dependent manner, thus indicating stability and antitumor activity in vivo. Such bispecific HexAbs may constitute a new class of therapeutic agents for improved cancer immunotherapy, as shown here for MCL and other $CD20^+/CD74^+$ malignancies. (*Blood*. 2012;119(16): 3767-3778)

Introduction

mAbs are gaining an increasing role in the therapy of cancer, and their efficacy can be enhanced when combined with other modalities, including the use of additional Abs binding to different targets.[1-3] In principle, combination Ab therapy can be accomplished with a single bispecific Ab (bsAb) to avoid the need for administering 2 different Abs sequentially, which is time consuming, expensive, and inconvenient. Hence, efforts are being directed toward developing bsAbs as a new class of Ab-based therapeutics by generating various constructs differing in design, structure, and Ag-binding properties.

Depending on the built-in dual specificity, a bsAb may serve to recruit effector cells or effector molecules to target cells, or it may improve the target selectivity by concurrent ligation of 2 different Ags expressed on the same cell, preferably associated with 2 different signaling pathways and mechanisms controlling cell proliferation. Thus, a desirable bsAb could overcome single-pathway resistance and could also enhance functional affinity, leading to increased retention on the bound cells and, probably, a higher potency, and, as a result, might be active against a human cancer that is poorly responsive to either parental mAb alone.

Mantle cell lymphoma (MCL) is an aggressive subtype of B-cell non-Hodgkin lymphoma (NHL) generally having a poor prognosis. Currently, there is no established standard of care, and the anti-CD20 mAb, rituximab, has shown a limited role in this disease despite MCL expressing CD20.[4-9] Accordingly, there is a need to develop new targeted therapeutics to treat this disease.[10] CD74 is a nonpolymorphic, type II transmembrane protein with diverse functions, which include serving as the receptor for macrophage migration-inhibitory factor[11] and mediating the trafficking of MHC class II for Ag presentation.[12] Enhanced expression of CD74 has been observed on malignant B cells and in other cancers, such as renal,[13] pancreatic,[14] and prostate,[15] making it an attractive target for immunotherapy.[16] More recently, the potential advantage of targeting both CD20 and CD74 has been reported by us in a preclinical study that involved rituximab and milatuzumab (humanized anti-CD74 IgG_1, also referred to as hLL1), which in the presence of a crosslinking Ab showed improved antitumor activity in MCL lines and primary patient samples compared with either parental Ab alone.[17]

The Dock-and-Lock (DNL) method is a platform technology that combines genetic engineering with site-specific conjugation to enable self-assembly of 2 modular components with each other, resulting in a covalent structure of defined composition with retained bioactivity.[18,19] We have applied DNL to generate various multivalent, multispecific structures that include monospecific and bispecific HexAbs, each comprising a pair of stabilized dimers of Fab linked to a full IgG at the carboxyl termini of the 2 heavy chains, thus conferring 6 Fab-arms and a common Fc entity.[20-22] To identify these HexAbs, we assign each of them a code of X-(Y)-(Y), where X and Y are specific numbers given to differentiate the Abs, and a designated number enclosed in parentheses representing the Ab as a stabilized Fab dimer. For example,

Submitted September 23, 2011; accepted January 17, 2012. Prepublished online as *Blood* First Edition paper, January 23, 2012; DOI 10.1182/blood-2011-09-381988.

There is an Inside *Blood* commentary on this article in this issue.

The online version of this article contains a data supplement.

The publication costs of this article were defrayed in part by page charge payment. Therefore, and solely to indicate this fact, this article is hereby marked "advertisement" in accordance with 18 USC section 1734.

Table 1. HexAbs used in the study

Designation		CH_3-AD2-IgG module		CH_1-DDD2-Fab module	
Current	Previous	Ab	Ag	Ab	Ag
20-(74)-(74)	NA	Veltuzumab	CD20	Milatuzumab	CD74
74-(20)-(20)	NA	Milatuzumab	CD74	Veltuzumab	CD20
74-(74)-(74)	NA	Milatuzumab	CD74	Milatuzumab	CD74
20-(20)-(20)	20-20	Veltuzumab	CD20	Veltuzumab	CD20
20-(22)-(22)	20-22	Veltuzumab	CD20	Epratuzumab	CD22
22-(20)-(20)	22-20	Epratuzumab	CD22	Veltuzumab	CD20

20-(74)-(74) designates the bispecific HexAb comprising a divalent anti-CD20 IgG of veltuzumab (also referred to as hA20) and a pair of stabilized dimers of Fab derived from milatuzumab. The designations of various HexAbs relevant to this study, which include 20-(74)-(74), 74-(20)-(20), 74-(74)-(74), 20-(20)-(20), 20-(22)-(22), and 22-(20)-(20), along with their modular components, are provided in Table 1.

In our initial efforts in developing HexAbs from veltuzumab and epratuzumab (anti-CD22 IgG),[20-22] we found the bispecific 20-(22)-(22) and 22-(20)-(20) induced growth inhibition and caspase-independent apoptosis in Burkitt lymphoma lines (Daudi, Raji, and Ramos) in the absence of a crosslinking Ab, which is often required for the parental Abs to be effective in vitro. Such direct cytotoxicity, however, was not observed in JeKo-1, a MCL line expressing comparable levels of CD20 and CD22 as Daudi NHL.

In this study, we describe, for the first time, the successful generation and characterization of 3 novel HexAbs from veltuzumab (hA20) and milatuzumab (hLL1), namely 20-(74)-(74), 74-(20)-(20), and 74-(74)-(74). We demonstrate that the bispecific HexAbs, 20-(74)-(74) and 74-(20)-(20), unlike anti-CD20/CD22 bsAbs, are highly cytotoxic in 3 blastoid MCL lines, JeKo-1,[23] Granta-519,[24] and Mino,[25] as well as in primary tumor cells from patients with MCL or chronic lymphocytic leukemia (CLL), all of which respond poorly to anti-CD20 or anti-CD74 mAbs alone in the absence of a crosslinking Ab. Selective experiments to interrogate the intracellular events triggered by juxtaposing CD20 and CD74, which could conceivably result only from coligating both CD20 and CD74 with a bsAb or crosslinking the 2 parental Abs with a secondary Ab, showed the prominent roles of actin reorganization and lysosomal membrane permeabilization (LMP) in the mechanisms of cell death.

Methods

Cell lines, Abs, and reagents

The cell lines used in the study were obtained as follows: Daudi, Raji, JeKo-1, and Mino from ATCC; Granta-519, MEC-1, MN-60, KMS-12-BM, KMS-12-PE, and REH from DSMZ; WAC, CAG, and KMS-11 from Dr Rhona Stein (Garden State Cancer Center). Tositumomab and rituximab were obtained commercially. Phospho-specific and other Abs were acquired from Cell Signaling. Cell culture media, supplements, annexin V Alexa Fluor 488 conjugate, tetramethylrhodamine ethyl ester (TMRE), LysoTracker Red DND-99, CM-H_2DCF-DA, DAPI, Alexa Fluor 568 phalloidin, and acridine orange were from Invitrogen. One Solution Cell Proliferation assay reagent was obtained from Promega. Phosphosafe buffer, latrunculin B, cytochalasin D, bafilomycin A1, and concanamycin A were procured from EMD Chemicals. Magic Red Cathepsin B assay kit was purchased from ImmunoChemistry Technologies. All other chemicals were obtained from Sigma-Aldrich.

Cell culture

Malignant cell lines were cultured at 37°C in 5% CO_2 in RPMI 1640 medium supplemented with 10% heat-inactivated FBS, 2mM L-glutamine, 200 U/mL penicillin, and 100 μg/mL streptomycin. Cells from patients with CLL and from patients with MCL were isolated from peripheral blood by Ficoll-Hypaque separation and stored frozen at −70°C. For experimental analysis, cells were thawed, grown in RPMI media containing 10% FBS and antibiotic supplements, and treated with the reagents as indicated. All patients gave written, informed consent under a protocol approved by the institutional review board at The Ohio State University or Weill-Cornell Medical College.

Cytotoxicity assay

Cells were seeded in 48-well plates (5×10^4 cells per well) and incubated with each test article at a final concentration of 0.006nM-100nM for 4 days. The number of viable cells was then determined with the MTS assay per the manufacturer's protocol, plotted as percentage of the untreated, and analyzed by Prism Version 4.03 software.

Immunoblot analysis

JeKo-1 cells (3.6×10^7 cells) were treated with each test article at 10nM for a predetermined time. Cells were washed with PBS, pelleted by centrifugation and lysed in ice-cold phosphosafe buffer, and the lysate was clarified by centrifugation at 13 000*g*. Protein samples (20 μg/lane) were resolved by SDS-PAGE on 4%-20% gradient tris-glycine gels and transferred onto nitrocellulose membranes, which were probed with suitable Abs and visualized with enhanced chemiluminescence, as described.[22]

Assessment of $\Delta\psi_m$ and ROS

Flow cytometry was used to determine mitochondrial membrane potential ($\Delta\psi_m$) and reactive oxygen species (ROS). Briefly, cells in 6-well plates (2×10^5 cells per well) were treated with each test article at 10nM for 48 hours, washed, and stained for 30 minutes in the dark at 37°C with TMRE (50nM) for $\Delta\psi_m$ or CM-H_2DCF-DA (1μM) for ROS. Samples were then washed with PBS and analyzed.

Annexin V binding assay

Cells in 6-well plates (2×10^5 cells per well) were treated with each test article at 10nM for 24-72 hours as indicated, washed, resuspended in 100 μL of annexin V binding buffer (10mM HEPES, 140mM NaCl, and 2.5mM $CaCl_2$ in PBS), stained with 5 μL of annexin V–Alexa Fluor 488 conjugate for 20 minutes, then with 1 μg/mL propidium iodide (PI) in 400 μL of annexin binding buffer, and analyzed by flow cytometry. Cells stained positive with annexin V (including both PI^- and PI^+) were counted as apoptotic populations. When required, cells were pretreated with the indicated inhibitors for 2 hours before adding the test article.

Nuclear extracts

JeKo-1 cells (3.6×10^7 cells) were treated with each test article at 10nM for 72 hours. Cytosolic and nuclear extracts were fractionated as described.[26] Equal amounts of nuclear and cytosolic proteins (10 μg) were resolved by SDS-PAGE and probed for NF-κB protein p65, Brg-1, and β-actin, with the latter 2 serving as loading controls for nuclear and cytosolic proteins, respectively.

Assessment of lysosomal changes and cathepsin B release

To determine the changes in lysosomal volumes, 2×10^5 cells per well in 6-well plates were treated with each test article at 10nM for 48 hours. After washing, cells were labeled with LysoTracker Red DND-99 (75nM) followed by incubation in the dark at 37°C for 1 hour. Cells were washed with PBS and analyzed by flow cytometry. To evaluate LMP, JeKo-1 cells were treated with select Abs at 10 μg/mL for 4 hours, labeled with acridine orange, and examined by fluorescence microscopy. To study cathepsin B release, JeKo-1 cells were treated with select Abs (10nM) for 48 hours,

fixed with 4% paraformaldehyde, permeabilized with 0.1% Triton X-100, costained with Magic Red Cathepsin B and DAPI, and examined by fluorescence microscopy.

Ex vivo depletion of JeKo-1 and B cells from whole blood

Blood from healthy volunteers was obtained under a protocol approved by the New England Institutional Review Board. JeKo-1 cells (5×10^4) were mixed with heparinized whole blood (150 μL) and incubated with various concentrations of each test article for 2 days at 37°C and 5% CO_2. After lysing the red blood cells and washing, the remaining cells were stained with FITC–anti-CD19, PE–anti-CD14, or allophycocyanin-conjugated mouse IgG_1 isotype control and analyzed by flow cytometry. JeKo-1 cells and monocytes were identified in the monocyte gate as $CD19^+$ and $CD14^+$ populations, respectively. Normal B cells are $CD19^+$ in the lymphocyte gate.

In vivo efficacy

Female 8-week-old SCID mice (Taconic Farms) comprising 7 different treatment groups of 8 mice each were inoculated intravenously with JeKo-1 (2.5×10^7 cells). After 7 days, one group received 370 μg of 20-(74)-(74) intraperitoneally twice weekly for 2 weeks. A second group received 74-(20)-(20) with the same dose and schedule. Two lower doses (37 μg and 3.7 μg) also were examined for each HexAb with the same schedule and injection route. The control group received saline. The mice were observed daily for signs of distress or paralysis, weighed weekly, and killed humanely when they developed hind-limb paralysis, became moribund, or lost > 20% of initial body weight. Animal studies were performed under protocols approved by the Institutional Animal Care and Use Committee at the Center for Molecular Medicine and Immunology.

Statistical analysis

For in vitro studies, comparisons of mean values between 2 treatments were determined by Student *t* test, assuming a normal distribution for the data. A 1-tailed *t* test was used when a particular treatment was compared with untreated populations, and a 2-tailed *t* test was used comparing 2 differently treated samples. For in vivo studies, comparisons of survival curves used the log-rank test for the data. $P < .05$ was considered statistically significant.

Results

Generation of HexAbs and demonstration of direct cytotoxicity in vitro

The generation of monospecific and bispecific HexAbs by the DNL method from cognate C_H3-AD2-IgG-X and C_H1-Fab-DDD2-Y, where X and Y can be either hLL1 (milatuzumab) or hA20 (veltuzumab), is shown in Figure 1. These HexAbs were purified to near homogeneity, as indicated by SDS-PAGE and size exclusion HPLC analyses (supplemental Figure 1, available on the *Blood* Web site; see the Supplemental Materials link at the top of the online article) for 20-(74)-(74) and 74-(20)-(20), and were evaluated in a panel of cell lines with various expression levels of CD20 and CD74 (Table 2). Note that both 20-(74)-(74) and 74-(20)-(20) depicted stronger binding to the 3 MCL cell lines (JeKo-1, Granta-519, and Mino) than their parental Abs (data not shown). In the cell proliferation assays (Figure 2A), the 2 bispecific anti-CD20/CD74 HexAbs showed potent cytotoxicity against JeKo-1, Granta-519, Mino, and Raji, with the EC_{50} in the nanomolar range. In comparison, we observed < 20% (Granta-519 and Raji) and < 50% (JeKo-1 and Mino) of growth inhibition when both parental Abs were combined at the highest concentration tested (100nM). Additional results showed that the antiproliferative activity of the monospecific 74-(74)-(74) and 20-(20)-(20) HexAbs, as well as the bispecific anti-CD20/CD22 HexAb, 20-(22)-(22), paralleled that of

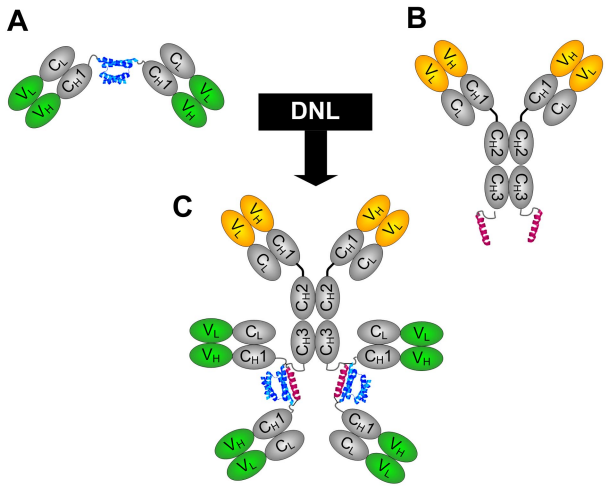

Figure 1. Schematic structures of DNL modules and HexAb. (A) The design of C_H1-DDD2-Fab module. (B) The design of C_H3-AD2-IgG module. (C) The structure of bispecific HexAb construct generated by DNL from reacting C_H3-AD2-IgG and C_H1-DDD2-Fab. The DDD2 and AD2 are shown in blue and red, respectively.

combined hLL1 and hA20 in JeKo-1, and thus was considerably lower in activity than the bispecific anti-CD20/CD74 HexAbs (Figure 2B). However, notable cytotoxicity of 20-(20)-(20) was found in Mino and Granta-519, and an initial survey showed cell lines derived from CLL (WAC and MEC-1), acute lymphocytic leukemia (REH and MN-60), and multiple myeloma (RPMI8226, CAG, KMS-11, KMS-12-BM, and KMS-12-PE) were relatively resistant (EC_{50} > 100nM) to the anti-CD20/CD74 HexAbs. For both 20-(74)-(74) and 74-(20)-(20), the addition of either parental Ab at a moderate concentration of 10 μg/mL partially reduced their antiproliferative effects in JeKo-1 (Figure 2C), suggesting the requirement of juxtaposing CD20 and CD74 for maximal cytotoxicity. A list of the EC_{50} values is provided in the supplemental Table 1.

Involvement of apoptosis

The ability of 20-(74)-(74) and 74-(20)-(20) to induce apoptosis was evaluated by flow cytometry with the use of the annexin V binding assay. In JeKo-1 (Figure 3A), Granta-519 (Figure 3B) and Mino (Figure 3C), both bispecific anti-CD20/CD74 HexAbs at 10nM showed a statistically significant increase in annexin V^+ cells compared with untreated cells ($P < .016$), cells treated with

Table 2. Expression of CD20 and CD74 as determined by hA20 and hLL1, respectively, in cell lines used in the study

	Mean fluorescence intensity		
	FITC control	CD20	CD74
JeKo-1	4	161	11
Mino	3	697	98
Granta-519	3	1734	53
Daudi	6	483	60
Raji	4	960	310
RPMI8226	5	25	10
KMS-12PE	4	4	23
KMS-12BM	4	590	58
KMS-11	7	17	96
CAG	5	4	139

Ag expression analysis was done by indirect immunofluorescence staining. Cells were incubated with 10 μg/mL amounts of hA20 and hLL1 for CD20 and CD74 expression analysis, respectively, for 45 minutes followed by FITC-conjugated $F(ab')_2$ fragment goat anti-human Fc-specific secondary antibody. All incubations were done on ice followed by washing and flow cytometric analysis.

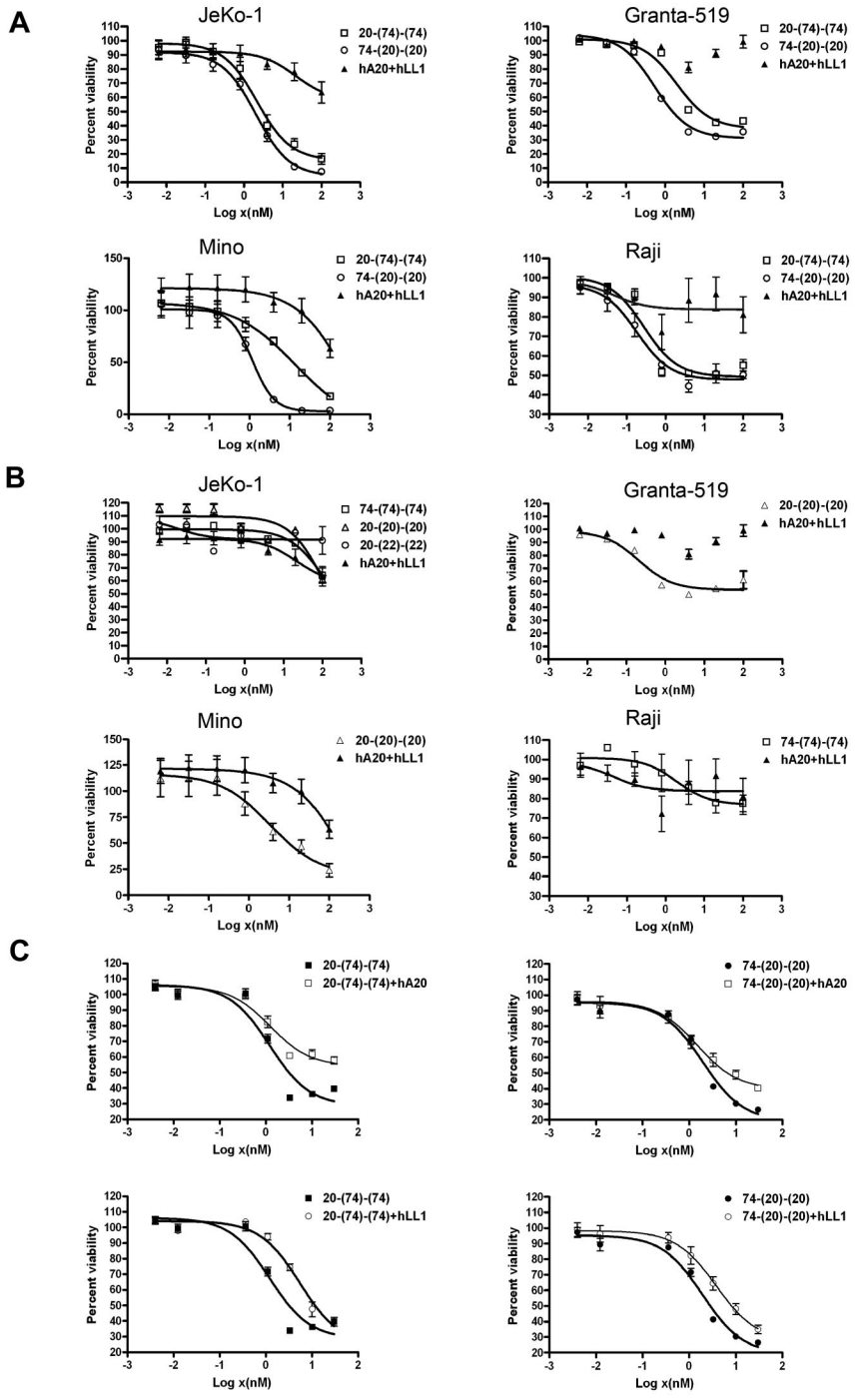

Figure 2. Direct cytotoxicity induced by anti-CD20/CD74 HexAbs in NHL cell lines as determined by the MTS assay. (A) JeKo-1, Granta-519, Mino, and Raji (5×10^4 cells per well in 48-well plate) cells were treated with indicated concentrations of Abs for 4 days. (B) Effect of monospecific 20-(20)-(20) on JeKo-1, Granta-519, and Mino cells; bispecific 20-(22)-(22) on JeKo-1 cells; and monospecific 74-(74)-(74) on Raji cells. (C) Dose-response curves showing partial inhibition of 20-(74)-(74) and 74-(20)-(20) in JeKo-1 cells by excess hA20 or hLL1 (10 μg/mL). Error bars represent (SD); n = 3.

either parental Ab ($P < .031$), and cells treated with both parental Abs combined ($P < .033$). Statistically significant increases of 10%-25% in annexin V^+ cells were also observed for each of 4 MCL patient samples ($P < .008$; Figure 3D) and 6 of 7 CLL patient specimens ($P < .015$; Figure 3E) compared with untreated samples, as well as for 3 of 4 MCL patient samples ($P < .025$) and 4 or 5 of 7 CLL patient samples ($P < .04$) compared with parental mAbs combined.

We also evaluated the effects of 20-(74)-(74) and 74-(20)-(20) on selective apoptotic and antiapoptotic proteins. The immunoblot results indicate that treatment of JeKo-1, Granta-519, and Mino, with both HexAbs substantially reduced Bcl-xL, but had no apparent effect on Bcl-2, Mcl-1, and Bax (Figure 4A). The observed apoptosis was caspase independent, as evidenced by the lack of appreciable changes in the expression level or cleavage of caspase 3, caspase 8, and caspase 9 in JeKo-1 (Figure 4B), and the absent activity of the pan-caspase inhibitor z-vad-fmk (Figure 4C). This caspase-independent apoptosis was associated with 20%-30% more cells showing a lower $\Delta\psi_m$ and ~ 30% increase in ROS in Granta-519 (Figure 4D) and somewhat less in JeKo-1 (supplemental Figure 2).

HA and actin reorganization

As shown in Figure 5A, 20-(74)-(74) and 74-(20)-(20), but not the parental Abs, evoked in JeKo-1 a strong homotypic adhesion (HA),

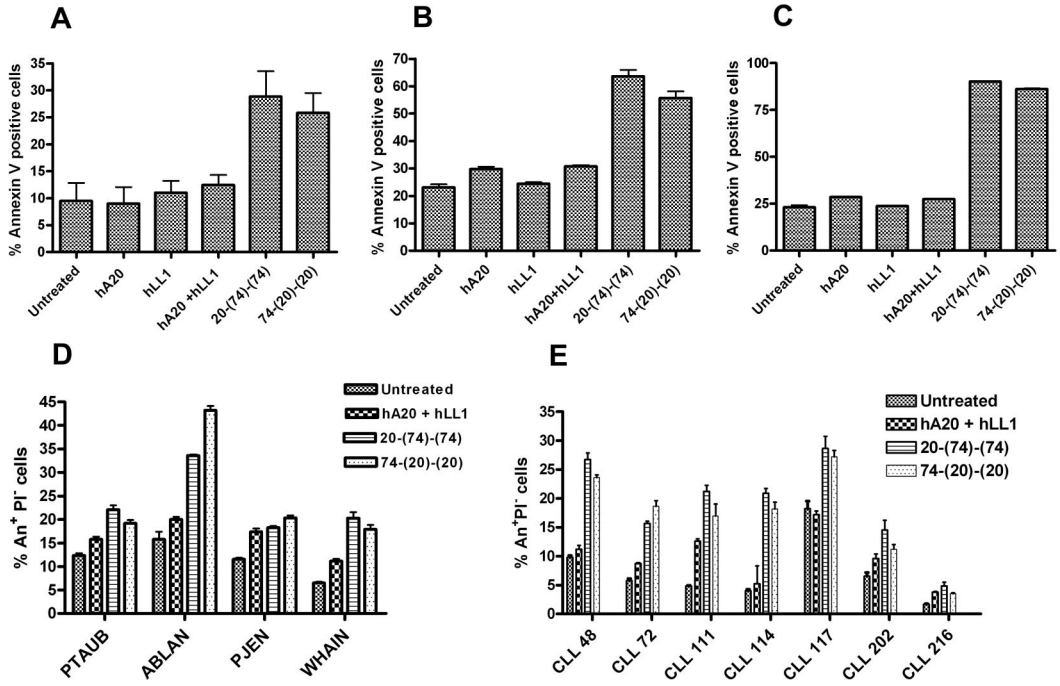

Figure 3. Induction of apoptosis by anti-CD20/CD74 HexAbs. (A) JeKo-1, (B) Granta-519, and (C) Mino cells (2×10^5 cells per well in 6-well plate) were treated with 10nM of indicated Abs for 48 hours followed by annexin staining analysis. The 2 bispecific anti-CD20/CD74 HexAbs induced statistically significant apoptosis in all 3 cell lines compared with cells treated or not treated with parental Abs, alone or combined. (D) Annexin analysis on primary samples from patients with MCL treated with indicated Abs (10nM) for 24-48 hours. (E) Annexin analysis on primary samples from patients with CLL treated with indicated Abs (10nM) for 24-48 hours. (D-E), Data are shown as annexin$^+$ PI$^-$ cells (early apoptosis). The 2 anti-CD20/CD74 HexAbs induced statistically significant early apoptosis in MCL and CLL compared with the untreated controls. One of the patient samples (CLL 216) did not respond to any treatment. Error bars represent SD (A-E); n = 3.

which was prevented by latrunculin B, an inhibitor of actin polymerization. Similar results were observed for Granta-519, Mino, and Raji (data not shown). Considerable HA (> 40%) also could be induced by the bispecific anti-CD20/CD74 HexAbs in JeKo-1, but not in KMS-11 (a CD20$^-$ multiple myeloma line expressing a high level of CD74), by tositumomab (murine anti–human CD20 IgG_{2a}, also referred to as B1) alone, or by the parental Abs in the presence of a crosslinking Ab (supplemental Table 2). Pretreatment of JeKo-1 with cytochalasin D (another inhibitor of actin polymerization), which is less toxic than latrunculin B, thus allowing longer incubation, decreased the extent of annexin V$^+$ cells (Figure 5B) from 21% ± 1% to 13% ± 2% ($P < .02$) by 20-(74)-(74) or from 23% ± 2% to 16% ± 1% ($P < .025$) by 74-(20)-(20). These results correlate HA and actin reorganization with apoptosis in cell lines sensitive to the bispecific anti-CD20/CD74 HexAbs. Additional studies in JeKo-1 showed that treatment with 20-(74)-(74) or 74-(20)-(20) induced actin to cluster at the cell-cell junction, and similar results could be produced either with B1 in the absence of a crosslinking Ab or with rituximab, veltuzumab, or milatuzumab in the presence of a crosslinking Ab (supplemental Figure 3A-B). However, neither 20-(74)-(74) nor 74-(20)-(20) appeared to colocalize with actin at the cell-cell junction when cells were costained with FITC-conjugated anti–human-Fc, which also showed that 20-(74)-(74) was actively internalized, whereas 74-(20)-(20) remained localized at the cell surface (supplemental Figure 3C).

Involvement of lysosomes

The HexAb-mediated apoptosis could be reduced effectively with concanamycin A or bafilomycin A1, both functioning by blocking lysosomal acidification through selective inhibition of the V-type ATPase.[27] As shown in Figure 5C, treatment of JeKo-1 with concanamycin A (10nM) or bafilomycin A1 (50nM) before the addition of either 20-(74)-(74) or 74-(20)-(20) largely decreased the extent of annexin V$^+$ cells. Further, a sizable enlargement of the lysosomal compartments by the 2 bispecific anti-CD20/CD74 HexAbs was shown (Figure 5D) with the use of flow cytometry with a fluorescent acidotropic probe, LysoTracker Red DND-99. These results implicate a causal role of lysosomes in cell death and are supported by fluorescence microscopic evidence of LMP (supplemental Figure 4) and release of cathepsin B into the cytosol (Figure 5E).

Effect on MAP kinases, Src, p65/NF-κB, and Akt

On the basis of our previous work on IMMU-114, a humanized anti–HLA-DR mAb[28] and the abundant literature pertaining to the signaling transduction pathways of Abs targeting CD20 (see Vega et al[29]), we opted to assess the roles of MAP kinases, Src, p65/NF-κB, and Akt in Jeko-1 after the colligation of CD74 and CD20. As shown for 74-(20)-(20) and 20-(74)-(74) in the top and middle panels of Figure 6A, both HexAbs induced rapid and sustained activation of ERK and JNK kinases in JeKo-1, which could be detected within 30 minutes, persisted for the next 6 hours, and returned to basal levels by 24 hours. In contrast, no phosphorylation of ERKs and JNK was observed in those cells incubated with both parental Abs (Figure 6A bottom panel). Activation of ERKs and JNK was not affected by pretreating the cells with 10μM latrunculin B (supplemental Figure 5). Because of high constitutive phosphorylation of the p38 MAP kinase in JeKo-1, we were unable to determine any change on treatment with the bispecific HexAbs. Pertinent results include the ability of both HexAbs to induce a larger decrease (~ 60%) of upstream phospho-Src than that of the

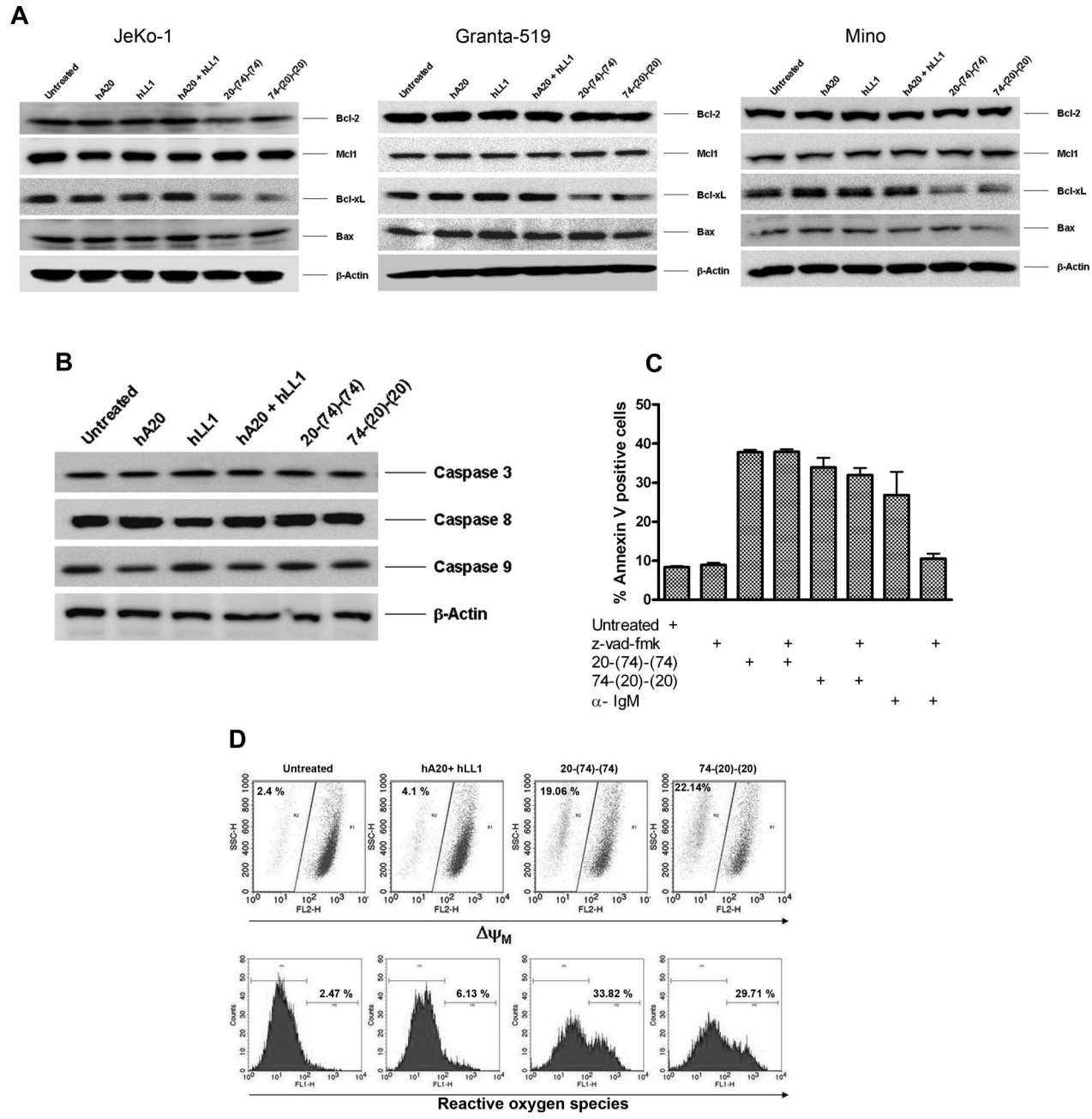

Figure 4. Anti-CD20/CD74 HexAbs induce stress- and caspase-independent apoptosis in target cells. (A) Western blot analysis of select antiapoptotic and proapoptotic proteins on treatment with 10nM of indicated Abs for 48 hours in JeKo-1, Granta-519, and Mino cells. The 2 anti CD20/CD74 HexAbs down-regulated the antiapoptotic protein Bcl-xL. (B) Neither 20-(74)-(74) nor 74-(20)-(20) activated caspase 3, caspase 8, and caspase 9 in JeKo-1. (C) Caspase inhibitor z-vad-fmk did not inhibit the apoptosis in JeKo-1 induced by anti-CD20/CD74 HexAbs. JeKo-1 cells were pretreated with z-vad-fmk pan caspase inhibitor (10μM) for 2 hours followed by treatment with 10nM of indicated Abs or anti-IgM (10 μg/ mL, a positive control for caspase-dependent apoptosis) for 72 hours, and apoptosis was determined by annexin V staining. Error bars represent SD; n = 3. (D) Both anti-CD20/CD74 HexAbs induced changes in mitochondrial membrane potential (top panel) and generated ROS (bottom panel) in Granta-519 cells.

parental hA20 mAb (~ 30%), as shown in Figure 6B, and to inhibit the downstream nuclear translocation of p65/NF-κB (Figure 6C). We also observed that the bispecific HexAbs notably reduced the level of constitutively activated Akt in JeKo-1 (Figure 6D).

Ex vivo depletion of JeKo-1 and normal B cells from human whole blood

The effect of 20-(74)-(74) and 74-(20)-(20) on Jeko-1 and normal B cells was evaluated ex vivo with the use of human whole blood spiked with JeKo-1, which may better mimic the activity in patients with MCL. When evaluated at high concentrations (10nM and 25nM) in whole blood spiked with JeKo-1 cells, we observed > 90% depletion of JeKo-1 cells with 20-(74)-(74), hA20, and hA20 + hLL1, but ≤ 50% depletion with 74-(20)-(20), and < 20% depletion with hLL1 or the nontargeting hMN-14 (anti-CEACAM5) isotype-control Ab (Figure 7A left panel). The depletion of normal B cells, however, was similar for the 2 HexAbs, in the range of 50%-70% for 20-(74)-(74) and 60%-75% for 74-(20)-(20), with higher depletion (80%-90%) attained by hA20 or the combination of hA20 and hLL1 (Figure 7A right panel). Representative dot plots

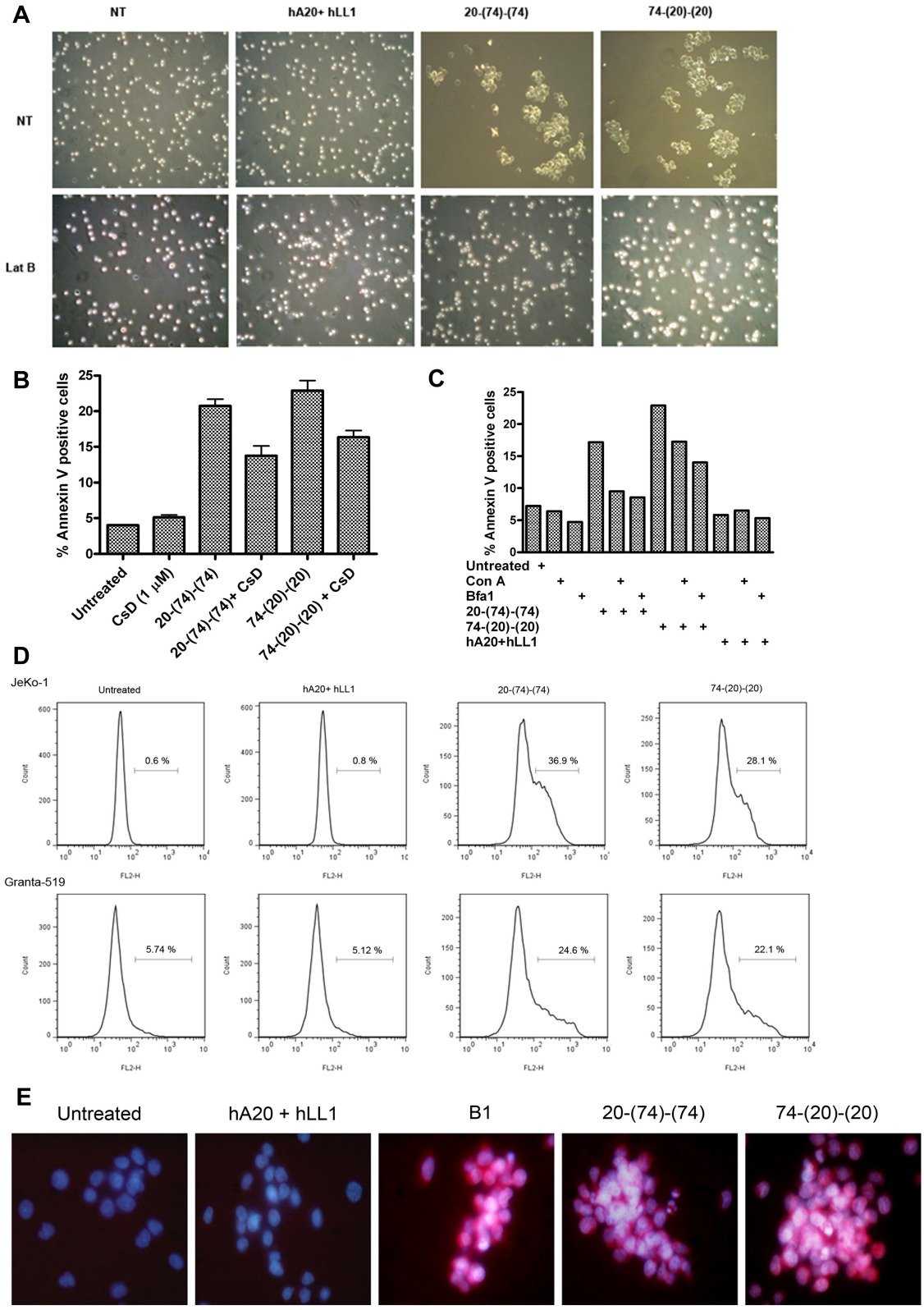

Figure 5. Correlation of homotypic adhesion, actin reorganization, and lysosomal involvement to cell death evoked by the bispecific anti-CD20/CD74 HexAbs. (A) JeKo-1 cells were pretreated or not pretreated with the actin polymerization inhibitor, latrunculin B (1μM), for 2 hours followed by addition of HexAbs or both parental mAbs and evaluated for aggregation after 4 hours by light microscopy. (B) Apoptosis induced by HexAbs was reduced significantly ($P < .025$) in JeKo-1 with 1μM cytochalasin D (CsD), another inhibitor of actin polymerization. Error bars represent SD; n = 3. (C) Lysosomal V ATPase inhibitors, concanamycin A (Con A) and bafilomycin A1 (Bfa1), inhibited the apoptosis induced by HexAbs in JeKo-1 cells. (D) HexAbs induced changes in lysosomal volumes as determined by staining the cells with LysoTracker (75nM). The lysosomal compartmental volume changes were analyzed for JeKo-1 cells (top panel) and Granta-519 (bottom panel) by flow cytometry as enhanced binding and shift in the emission spectrum toward the right. (E) Immunofluorescence analysis of cathepsin B staining (red) 48 hours after treatment with select Abs. Nuclei were stained with DAPI (blue).

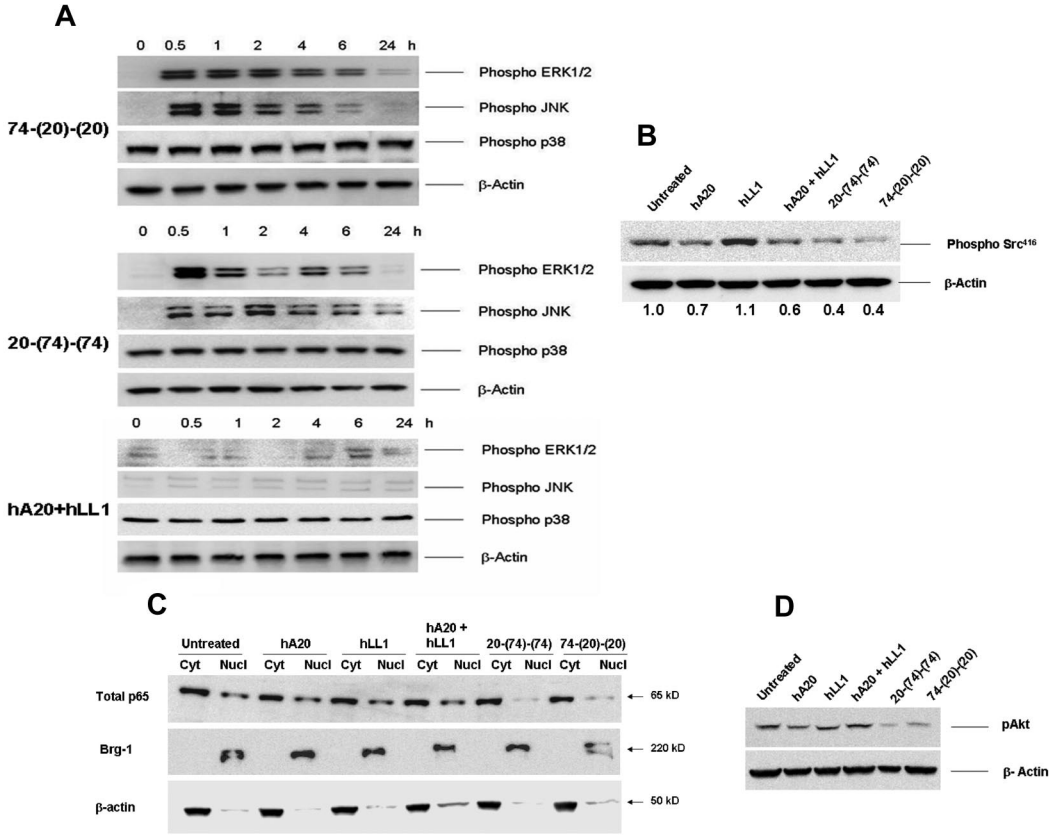

Figure 6. Anti-CD20/CD74 HexAbs inducing activation of ERK and JNK MAP kinases and inhibiting the Akt and NFκB signaling. (A) Rapid and sustained phosphorylation of ERK1/2 and JNK MAP kinases. JeKo-1 cells were treated with 10-nM concentrations of 74-(20)-(20) (top panel) or 20-(74)-(74) (middle panel) or with a combination of parental mAbs (bottom panel) for the indicated time points up to 24 hours. Cells were lysed, and samples were evaluated after probing with relevant Abs. β-actin was used as the loading control. (B) The CD20-targeting HexAbs, like veltuzumab, inhibited the phosphorylation of c-Src^{416}. (C) HexAbs inhibited the nuclear translocation of p65. JeKo-1 cells were treated with the indicated Abs for 72 hours, and nuclear and cytosolic extracts were prepared. Equal amounts of proteins were evaluated for the expression levels of p65 in cytosolic and nuclear fractions. Brg-1 (nuclear) and β-actin (cytosolic) served as loading controls. (D) HexAbs inhibited the phosphorylation of Akt. JeKo-1 cells were treated with the indicated Abs for 24 hours, lysed, and probed for pAkt (serine 473).

for ex vivo treatments with both anti-CD20/CD74 HexAbs are provided in the supplemental Figure 6. The apparently higher potency of 20-(74)-(74) compared with 74-(20)-(20) in depleting JeKo-1 cells from whole blood prompted subsequent studies with the use of 3 lower concentrations (0.1nM, 0.5nM, and 1nM), and the results shown in Figure 7B and C (left panels) confirmed the higher activity of 20-(74)-(74) than 74-(20)-(20) in depleting JeKo-1 cells from whole blood, because 20-(74)-(74) at 0.1nM was able to deplete 70% of JeKo-1 cells, whereas 74-(20)-(20) at 25nM could not achieve $>$ 50% depletion. The high potency of 20-(74)-(74) was also manifested by its ability to deplete 40%-50% of normal B cells at 0.1nM-1nM (Figure 7B right panel), a blood concentration that should easily be attainable clinically. Under the same conditions, 74-(20)-(20) at 0.1nM-1nM depleted $\leq$ 10% of normal B cells (Figure 7C right panel). It is noted that the ability of 20-(74)-(74) to deplete either JeKo-1 or normal B cells from whole blood is comparable, not superior, to that of hA20 or the combination of hA20 and hLL1

In vivo studies

To evaluate the efficacy of HexAbs in vivo, mice bearing disseminated JeKo-1 xenografts were treated with increasing doses (3.7, 37, or 370 μg) of either 20-(74)-(74) or 74-(20)-(20) given twice weekly for 2 weeks. Survival curves for the various treatment groups are shown in Figure 8. Saline control mice succumbed to disease progression by day 34. Both treatments at all 3 doses significantly improved survival compared with the control animals (P = .0001). Groups treated with the highest dose of 74-(20)-(20) had an ~ 30% increase in median survival over saline controls (43.5 days vs 34 days; P = .0001). A 60% increase in median survival time (53 days) over saline controls was observed in the group treated with 20-(74)-(74) at 370 μg (P = .0001). Both HexAbs given at 370 μg were more effective than the 2 lower doses ($P <$ .0143). However, no significant differences were observed between groups treated with 20-(74)-(74) and 74-(20)-(20) at the same dose. Although this study was not intended to disclose differences in the efficacy of the 2 bispecific HexAbs, they both showed dose-dependent effects.

Discussion

CD74 is the cell surface form of the HLA class II–associated invariant chain,[30] which plays a key role as a chaperone protein in Ag presentation by HLA-DR to T helper cells.[12,31] In addition, CD74 mediates macrophage migration inhibitory factor (MIF)–induced signal transduction as its cognate membrane receptor, resulting in activation of ERK1/2 and protection from p53-dependent apoptosis in a process that requires CD44 as a signaling

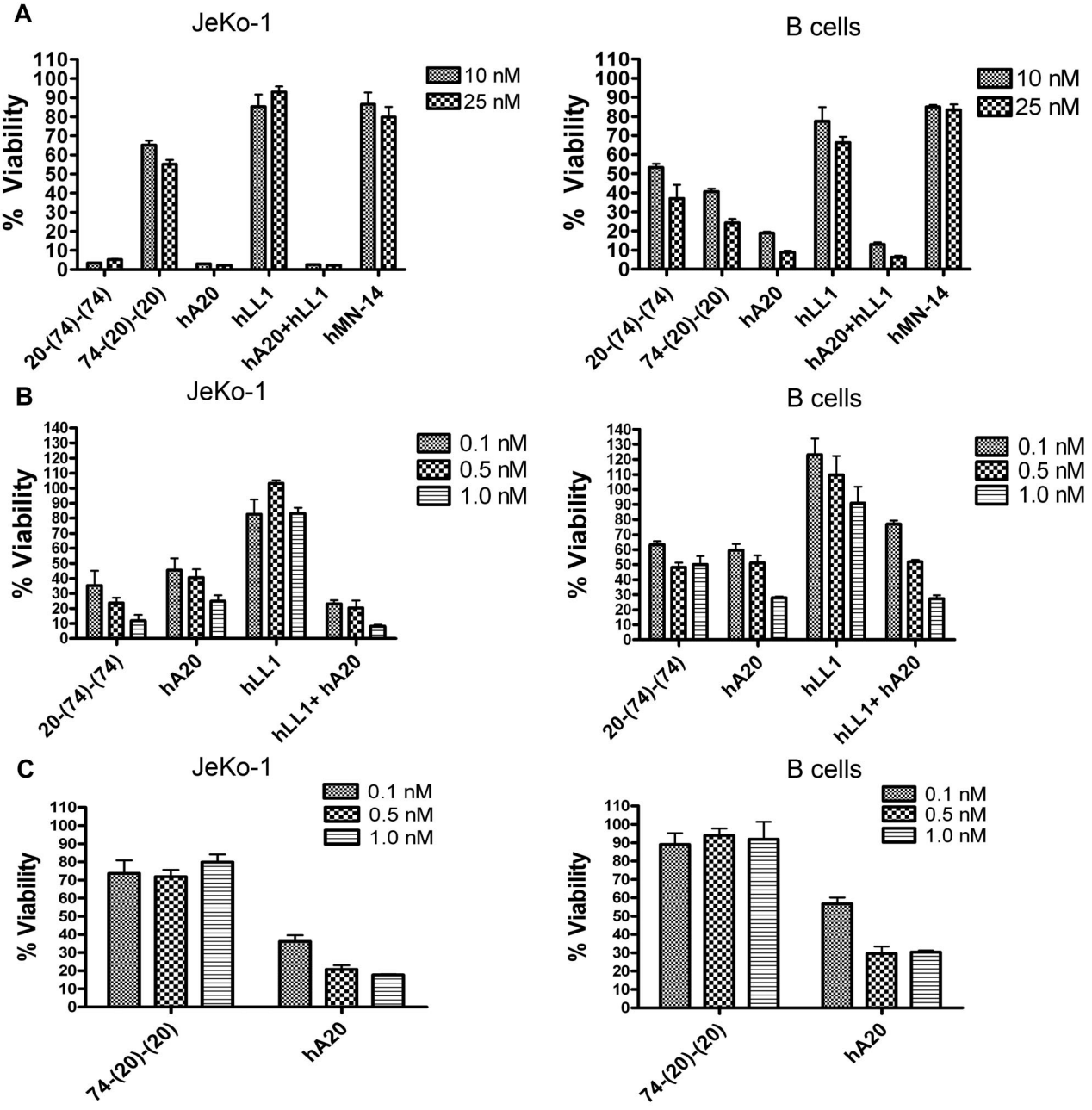

Figure 7. Activity of HexAbs in human blood ex vivo. The effect of the indicated Abs on the growth of spiked JeKo-1 cells in whole blood from a healthy volunteer was determined after 48 hours. JeKo-1 cells were analyzed as $CD19^+$ events in the monocyte gate. B cells were analyzed as $CD19^+$ events in the lymphocyte gate. Error bars represent SD; n = 3. (A) 20-(74)-(74) and 74-(20)-(20) were tested at 10nM and 25nM in JeKo-1 (left panel) and normal B cells (right panel). (B) 20-(74)-(74) was tested at 0.1nM, 0.5nM, and 1nM in JeKo-1 cells (left panel) and normal B cells (right panel). (C) 74-(20)-(20) was tested at 0.1nM, 0.5nM, and 1nM in JeKo-1 cells (left panel) and normal B cells (right panel).

component and involves PKA and c-Src.[32] Moreover, the intracellular domain of CD74 (CD74-ICD) released from intramembrane proteolysis in the endocytic compartments can activate NF-κB to induce B-cell maturation,[33] and this activity is further enhanced by stimulating CD74 with an agonistic Ab or MIF, either of which augments CD74-ICD release, increases Bcl-xL expression, and elevates the phosphorylation of both Akt and Syk.[34] In CLL cells and B lymphocytes, binding of CD74 to MIF initiates a signaling cascade that promotes cell survival by activation of NF-κB and secretion of IL-8, which can be inhibited by the antagonistic anti-CD74 mAb, milatuzumab,[35,36] thus further substantiating the rationale to develop milatuzumab-based therapeutic agents for the treatment of cancer[16] and autoimmune disease[37] by blocking the CD74/MIF pathway.

The commercial success of rituximab in treating certain B-cell malignancies and autoimmune disorders has stimulated much interest in developing new anti-CD20 Abs with improved efficacy, as well as elucidating the in vitro and in vivo mechanisms of action for rituximab and its analogues.[38] At present, next-generation anti-CD20 mAbs include human and humanized forms, with some claiming enhanced potency by Ab reengineering. Although CD20[39,40] is a well-validated therapeutic target and despite almost 15 years of clinical use of rituximab and an expansive amount of preclinical literature on the use of anti-CD20 mAbs in lymphoma

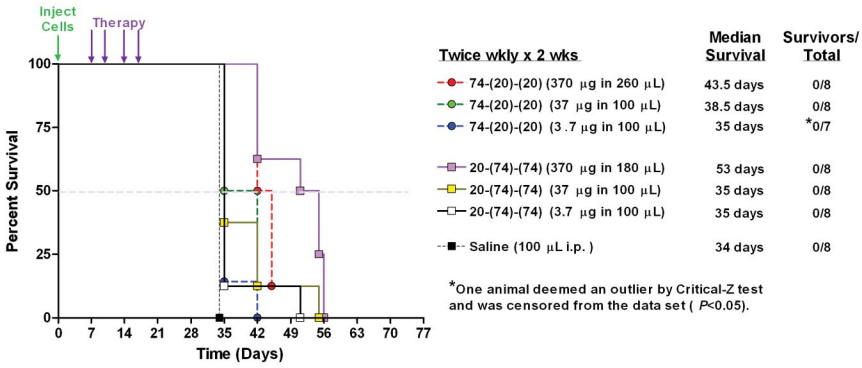

Figure 8. Therapeutic efficacy of HexAbs in disseminated JeKo-1 xenograft model. Seven groups of 8 mice (8-week-old female SCID mice) each were inoculated intravenously with JeKo-1 (2.5×10^7 cells per animal). After 7 days, 3 different does (ie, 370, 37, and 3.7 μg) of both HexAbs were administered by intraperitoneal injections twice a week for 2 weeks. Control mice received saline injections. 74-(20)-(20) and 20-(74)-(74), at the 370-μg dose level, resulted in 30% and 60% increases in median survival compared with saline controls, respectively.

models, how rituximab or other anti-CD20 mAbs kill lymphoma cells is still being debated[41] among the 3 principal mechanisms proposed: complement-dependent cytotoxicity (CDC), antibody-dependent cellular cytotoxicity (ADCC), and direct toxicity induced by signaling. Functional differences, as shown by a variety of assays such as induction of HA, stimulation of calcium mobilization, association with lipid rafts, capability for effective CDC or ADCC or both, and requirement of hypercrosslinking for direct in vitro cytotoxicity have been used[42] to classify anti-CD20 mAbs into type I, represented by rituximab, or type II, represented by tositumomab, with some data indicating that type II mAbs appear to outperform type I in preclinical models,[43,44] which awaits confirmation in patients. We have previously noted[20] that one effective approach to converting a type I anti-CD20 mAb to a type II can be achieved by making the type I mAb multivalent, as shown by the HexAb generated from the type I veltuzumab, 20-(20)-(20), which exhibits biologic properties attributable to both type II (eg, weak CDC; negative for calcium mobilization; positive for antiproliferation, apoptosis, and HA) and type I (eg, positive for trafficking to lipid rafts).[20]

The strategy to target both CD20 and CD74 with distinct mAbs was reported recently by us in a preclinical study that used a combination of milatuzumab and rituximab plus a crosslinking Ab in MCL lines and primary tumor cells,[17] which showed that the treatment resulted in rapid cell death, generation of ROS, loss of $\Delta\psi_m$, strong HA, and inhibition of p65 nuclear translocation. The observed cell death was attributed to a nonclassical apoptotic mechanism, because it lacked evidence of autophagy and caspase-activation but required the participation of actin and lysosomes. In the current study, we evaluated the potential of 2 anti-CD20/CD74 HexAbs for the therapy of MCL and observed similar intracellular events to those obtained with milatuzumab and rituximab combined in the presence of a crosslinking Ab, which include generation of ROS, loss of $\Delta\psi_m$, inhibition of p65 nuclear translocation, absence of autophagy (data not shown), and caspase-independence. The 2 anti-CD20/CD74 HexAbs, however, were capable of manifesting direct in vitro cytotoxicity, without the need for further crosslinking by a second Ab in 3 MCL (JeKo-1, Granta-519, and Mino) and 2 NHL cell lines (Daudi and Raji), as well as inducing a significantly higher number of annexin V^+ cells in tumor samples from patients with MCL and from patients with CLL compared with untreated controls.

We also investigated the signaling pathways triggered in JeKo-1 cells by the 2 anti-CD20/CD74 HexAbs. Our findings suggest that the rapid and sustained activation of ERKs and JNK may contribute to cell death,[45] as shown in Raji and SU-DHL4 treated with tositumomab and radiation,[46] in renal epithelial cells during oxidative injury,[47] and in Raji and other B-lymphoma lines (including JeKo-1 and Granta-519) on ligation to hL243 (anti-HLA-DR) mAb.[28] We also found that both anti-CD20/CD74 HexAbs disrupt the NF-κB pathway by inhibiting the translocation of p65 from cytosol to the nucleus and down-regulate pAkt and Bcl-xL, which may further promote cell death.

Ligation of various Abs with receptors such as HLA-DR, CD19, CD20, CD39, CD40, CD43, and others has been observed to induce HA in a panel of B-cell lymphoma lines.[48] The anti-CD20/CD74 HexAbs at 10nM induced very strong HA ($> 90\%$) in JeKo-1 cells. In contrast, in the absence of a crosslinking Ab, only little ($< 10\%$) or weak HA ($\sim 20\%$) was observed with either anti-CD20 or anti-CD74 mAbs alone and in combination. The HexAb-induced HA was blocked by inhibitors of actin polymerization, which also reduced cell death. Similar results have been observed with the combination of rituximab and milatuzumab in the presence of a crosslinking Ab in MCL lines.[17] Our studies also indicate that the induction of HA by the anti-CD20/CD74 HexAbs can be blocked without affecting the sustained activation of ERKs and JNK, and neither classic apoptosis nor autophagy is involved in the resulting cell death, which appeared to closely resemble the actin- and lysosome-dependent cell death evoked by tositumomab and hL243 in Raji and SU-DHL4.[49]

The present data also indicate that 20-(74)-(74), but not 74-(20)-(20), is internalized into JeKo-1; 74-(20)-(20) appeared to localize at the cell-cell junction. Thus, the direct in vitro cytotoxicity displayed by 20-(74)-(74) and 74-(20)-(20) is not modulated by internalization. Whether 20-(74)-(74) internalizes by the clathrin-dependent (coated pit) pathway, as shown for MIF/CD74,[50] and whether such internalization produces CD74-ICD, are interesting questions for future investigation.

Because of the differential susceptibility of 20-(74)-(74) and 74-(20)-(20) to internalization, it is probable that the initial events after ligation of CD20/CD74 by 20-(74)-(74) and 74-(20)-(20) are different but subsequently converge into actin reorganization, manifested externally as HA and internally as lysosomal membrane permeabilization, leading to caspase-independent cell death. We can further theorize as follows. In addition to crosslinking both CD74 and CD20, 74-(20)-(20) could link 4 CD20 molecules, which would be the same as using veltuzumab plus a crosslinking Ab, and thus should induce antiproliferation to a certain extent in target cells. Because there are more CD20 than CD74 molecules on the tested cells, when all CD74 sites are saturated by 74-(20)-(20), the remaining CD20 molecules can still be crosslinked by 74-(20)-(20) tetravalently to induce antiproliferation similar to the effect obtained with veltuzumab and a crosslinking Ab. For 20-(74)-(74), the influence on CD74 would be similar to milatuzumab plus a crosslinking Ab, but the effect on CD20 may be limited because only 2 CD20 molecules can be crosslinked. Thus, once all CD74

sites have been saturated, 20-(74)-(74) would exert little significance even with its binding to the remaining CD20 molecules. This may explain why 74-(20)-(20) appears to be slightly more potent than 20-(74)-(74) in vitro.

When examined ex vivo with the use of normal human blood spiked with JeKo-1 cells, 20-(74)-(74) at 0.1nM-1nM depleted these cells more effectively than veltuzumab at equivalent concentrations, whereas milatuzumab and 74-(20)-(20) at such concentrations did not show much activity. We attribute this improved efficacy to the ADCC and CDC effector functions of 20-(74)-(74), which are weaker or not measurable in 74-(20)-(20) (supplemental Figures 7-8). Both HexAbs, nevertheless, showed reduced but similar potency in depleting normal $CD19^+$ B cells, presumably because of a lower expression of CD20 or CD74 Ags, as well as the more mature type of peripheral B cell used.

In summary, bispecific anti-CD20/CD74 HexAbs, as represented by 20-(74)-(74) and 74-(20)-(20), were successfully generated, and their potential for therapy of a malignant tumor that is difficult to treat with single-mAbs, MCL, was shown in preclinical studies. The key findings are as follows. (1) Effective cell killing requires juxtaposing CD20 and CD74 in close proximity, which is achievable directly with the bispecific HexAbs or indirectly with the 2 parental mAbs in the presence of a crosslinking Ab. (2) The observed direct in vitro cytotoxicity is accompanied by extensive homotypic adhesion, relocation of actin to the cell-cell junction, notable lysosomal enlargement, release of cathepsin B into the cytosol, loss of $\Delta\psi_m$, generation of ROS, deactivation of the PI3K/Akt signaling pathway, and rapid and sustained activation of ERK and JNK MAPKs. (3) The bispecific HexAbs may affect these signaling pathways and actin reorganization independently and unrelated to their internalization properties. (4) HA can be a first indicator for determining whether a certain Ab or combination of Abs will display toxicity against Ag-expressing hematologic cells. Taking into consideration the in vitro activity of HexAbs, 74-(20)-(20) consistently shows more potency than 20-(74)-(74) when contributions from effector cells and complement are absent. However, this advantage is lost in the xenograft model, which may be because of ADCC and CDC activity. Thus, for clinical evaluation, both forms should be developed, correlating their effects to the expression of CD20 and CD74 by the lymphoma being investigated.

In conclusion, both 20-(74)-(74) and 74-(20)-(20) warrant further studies in additional B-cell malignancies, in particular MCL, and possibly in autoimmune diseases that involve B-cell immunity. These studies, as well as our prior work with anti-CD20/CD22 HexAbs, indicate that such bsAb constructs are more potent than either parental mAb or even combinations of these mAbs, and may thus constitute a new class of therapeutic Abs by invoking the juxtaposition and engagement of 2 independent targets on a cancer cell.

Acknowledgments

The authors thank Rosana Michel, John Kopinski, Anju Nair, and Roberto Arrojo for excellent technical assistance.

Authorship

Contribution: P.G. designed the research, performed experiments, analyzed data, and wrote the manuscript; D.M.G. conceived the project, reviewed the data, and wrote the manuscript; E.A.R. designed the research and analyzed data; T.M.C. designed the animal studies and analyzed the data; J.C.B. and N.M. provided clinical samples of MCL and reviewed the manuscript; R.R.F. provided patient samples of CLL and reviewed the manuscript; and C.-H.C. designed and supervised the research, reviewed the data, and wrote the manuscript.

Conflict-of-interest disclosure: P.G., E.R., T.C., C.-H.C., and D.M.G. have employment, stock, and/or stock options with Immunomedics Inc. The remaining authors declare no competing financial interests.

Correspondence: Chien-Hsing Chang, Immunomedics Inc, 300 American Rd, Morris Plains, NJ 07950; e-mail: kchang@immunomedics.com; or David M. Goldenberg, CMMI, Garden State Cancer Center, 300 American Rd, Morris Plains, NJ 07950; e-mail: dmg.gscancer@att.net.

References

1. Leonard JP, Coleman M, Ketas J, et al. Combination antibody therapy with epratuzumab and rituximab in relapsed or refractory non-Hodgkin's lymphoma. *J Clin Oncol.* 2005;23(22):5044-5051.
2. Strauss SJ, Morschhauser F, Rech J, et al. Multicenter phase II trial of immunotherapy with the humanized anti-CD22 antibody, epratuzumab, in combination with rituximab, in refractory or recurrent non-Hodgkin's lymphoma. *J Clin Oncol.* 2006;24(24):3880-3886.
3. Leonard JP, Schuster SJ, Emmanouilides C, et al. Durable complete responses from therapy with combined epratuzumab and rituximab: final results from an international multicenter, phase 2 study in recurrent, indolent, non-Hodgkin lymphoma. *Cancer.* 2008;113(10):2714-2723.
4. Lenz G, Dreyling M, Hoster E, et al. Immunochemotherapy with rituximab and cyclophosphamide, doxorubicin, vincristine, and prednisone significantly improves response and time to treatment failure, but not long-term outcome in patients with previously untreated mantle cell lymphoma: results of a prospective randomized trial of the German Low Grade Lymphoma Study Group (GLSG). *J Clin Oncol.* 2005;23(9):1984-1992.
5. Romaguera JE, Fayad L, Rodriguez MA, et al. High rate of durable remissions after treatment of newly diagnosed aggressive mantle-cell lymphoma with rituximab plus hyper-CVAD alternating with rituximab plus high-dose methotrexate and cytarabine. *J Clin Oncol.* 2005;23(28):7013-7023.
6. Inwards DJ, Fishkin PA, Hillman DW, et al. Long-term results of the treatment of patients with mantle cell lymphoma with cladribine (2-CDA) alone (95-80-53) or 2-CDA and rituximab (N0189) in the North Central Cancer Treatment Group. *Cancer.* 2008;113(1):108-116.
7. Lossos IS, Hosein PJ, Morgensztern D, et al. High rate and prolonged duration of complete remissions induced by rituximab, methotrexate, doxorubicin, cyclophosphamide, vincristine, ifosfamide, etoposide, cytarabine, and thalidomide (R-MACLO-IVAM-T), a modification of the National Cancer Institute 89-C-41 regimen, in patients with newly diagnosed mantle cell lymphoma. *Leuk Lymphoma.* 2010;51(3):406-414.
8. Sachanas S, Pangalis GA, Vassilakopoulos TP, et al. Combination of rituximab with chlorambucil as first line treatment in patients with mantle cell lymphoma: a highly effective regimen. *Leuk Lymphoma.* 2011;52(3):387-393.
9. Baiocchi RA, Alinari L, Lustberg ME, et al. Phase 2 trial of rituximab and bortezomib in patients with relapsed or refractory mantle cell and follicular lymphoma. *Cancer.* 2011;117:2442-2451.
10. Diefenbach CS, O'Connor OA. Mantle cell lymphoma in relapse: the role of emerging new drugs. *Curr Opin Oncol.* 2010;22(5):419-423.
11. Leng L, Metz CN, Fang Y, et al. MIF signal transduction initiated by binding to CD74. *J Exp Med.* 2003;197(11):1467-1476.
12. Landsverk OJ, Bakke O, Gregers TF. MHC II and the endocytic pathway: regulation by invariant chain. *Scand J Immunol.* 2009;70(3):184-193.
13. Young AN, Amin MB, Moreno CS, et al. Expression profiling of renal epithelial neoplasms: a method for tumor classification and discovery of diagnostic molecular markers. *Am J Pathol.* 2001;158(5):1639-1651.
14. Koide N, Yamada T, Shibata R, et al. Establishment of perineural invasion models and analysis of gene expression revealed an invariant chain (CD74) as a possible molecule involved in perineural invasion in pancreatic cancer. *Clin Cancer Res.* 2006;12(8):2419-2426.
15. Meyer-Siegler KL, Iczkowski KA, Vera PL. Further evidence for increased macrophage migration inhibitory factor expression in prostate cancer. *BMC Cancer.* 2005;5:73.
16. Stein R, Mattes MJ, Cardillo TM, et al. CD74: a

new candidate target for the immunotherapy of B-cell neoplasms. *Clin Cancer Res.* 2007;13(18 pt 2):5556s-5563s.

17. Alinari L, Yu B, Christian BA, et al. Combination anti-CD74 (milatuzumab) and anti-CD20 (rituximab) monoclonal antibody therapy has in vitro and in vivo activity in mantle cell lymphoma. *Blood.* 2011;117(17):4530-4541.
18. Rossi EA, Goldenberg DM, Cardillo TM, et al. Stably tethered multifunctional structures of defined composition made by the dock and lock method for use in cancer targeting. *Proc Natl Acad Sci U S A.* 2006;103(18):6841-6846.
19. Chang CH, Rossi EA, Goldenberg DM. The dock and lock method: a novel platform technology for building multivalent, multifunctional structures of defined composition with retained bioactivity. *Clin Cancer Res.* 2007;13(18 pt 2):5586s-5591s.
20. Rossi EA, Goldenberg DM, Cardillo TM, et al. Novel designs of multivalent anti-CD20 humanized antibodies as improved lymphoma therapeutics. *Cancer Res.* 2008;68(20):8384-8392.
21. Rossi EA, Goldenberg DM, Cardillo TM, Stein R, Chang CH. Hexavalent bispecific antibodies represent a new class of anticancer therapeutics, 1: Properties of anti-CD20/CD22 antibodies in lymphoma. *Blood.* 2009;113(24):6161-6171.
22. Gupta P, Goldenberg DM, Rossi EA, Chang CH. Multiple signaling pathways induced by hexavalent, monospecific, anti-CD20 and hexavalent, bispecific, anti-CD20/CD22 humanized antibodies correlate with enhanced toxicity to B-cell lymphomas and leukemias. *Blood.* 2010;116(17): 3258-3267.
23. Jeon HJ, Kim CW, Yoshino T, Akagi T. Establishment and characterization of a mantle cell lymphoma cell line. *Br J Haematol.* 1998;102(5): 1323-1326.
24. Jadayel DM, Lukas J, Nacheva E, et al. Potential role for concurrent abnormalities of the cyclin D1, p16CDKN2 and p15CDKN2B genes in certain B cell non-Hodgkin's lymphomas. Functional studies in a cell line (Granta 519). *Leukemia.* 1997; 11(1):64-72.
25. Lai R, McDonnell TJ, O'Connor SL, et al. Establishment and characterization of a new mantle cell lymphoma cell line, Mino. *Leuk Res.* 2002; 26(9):849-855.
26. Mayo MW, Norris JL, Baldwin AS. Ras regulation of NF-kappa B and apoptosis. *Methods Enzymol.* 2001;33373-33387.
27. Drose S, Altendorf K. Bafilomycins and concanamycins as inhibitors of V-ATPases and P-ATPases. *J Exp Biol.* 1997;200(Pt 1):1-8.
28. Stein R, Gupta P, Chen X, et al. Therapy of B-cell malignancies by anti-HLA-DR humanized monoclonal antibody, IMMU-114, is mediated through hyperactivation of ERK and JNK MAP kinase signaling pathways. *Blood.* 2010;115(25):5180-5190.
29. Vega MI, Huerta-Yepaz S, Garban H, et al. Rituximab inhibits p38 MAPK activity in 2F7 B NHL and decreases IL-10 transcription: pivotal role of p38 MAPK in drug resistance. *Oncogene.* 2004; 23(20):3530-3540.
30. Droken B, Moller P, Pezzutto A, Schwartz-Albiex R, Moldenhauer G. B-cell antigen: CD74. In: Knapp W, ed. *Leukocyte Typing IV: White Cell Differentiation Antigens.* Oxford, United Kingdom: Oxford University Press; 1989:106.
31. Weenink SM, Gautam AM. Antigen presentation by MHC class II molecules. *Immunol Cell Biol.* 1997;75(1):69-81.
32. Shi X, Leng L, Wang T, et al. CD44 is the signaling component of the macrophage migration inhibitory factor-CD74 receptor complex. *Immunity.* 2006;25(4):595-606.
33. Becker-Herman S, Arie G, Medvedovsky H, Kerem A, Shachar I. CD74 is a member of the regulated intramembrane proteolysis-processed protein family. *Mol Biol Cell.* 2005;16(11):5061-5069.
34. Starlets D, Gore Y, Binsky I, et al. Cell-surface CD74 initiates a signaling cascade leading to cell proliferation and survival. *Blood.* 2006;107(12): 4807-4816.
35. Binsky I, Haran M, Starlets D, et al. IL-8 secreted in a macrophage migration-inhibitory factor- and CD74-dependent manner regulates B cell chronic lymphocytic leukemia survival. *Proc Natl Acad Sci U S A.* 2007;104(33):13408-13413.
36. Shachar I, Haran M. The secret second life of an innocent chaperone: the story of CD74 and B cell/chronic lymphocytic leukemia cell survival. *Leuk Lymphoma.* 2011;52(8):1446-1454.
37. Borghese F, Clanchy FI. CD74: an emerging opportunity as a therapeutic target in cancer and autoimmune disease. *Expert Opin Ther Targets.* 2011;15(3):237-251.
38. Lim SH, Beers SA, French RR, et al. Anti-CD20 monoclonal antibodies: historical and future perspectives. *Haematologica.* 2010;95(1):135-143.
39. Pawluczkowycz AW, Beurskens FJ, Beum PV, et al. Binding of submaximal C1q promotes complement-dependent cytotoxicity (CDC) of B cells opsonized with anti-CD20 mAbs ofatumumab (OFA) or rituximab (RTX): considerably higher levels of CDC are induced by OFA than by RTX. *J Immunol.* 2009;183(1):749-758.
40. Mossner E, Brunker P, Moser S, et al. Increasing the efficacy of CD20 antibody therapy through the engineering of a new type II anti-CD20 antibody with enhanced direct and immune effector cell-mediated B-cell cytotoxicity. *Blood.* 2010;115(22): 4393-4402.
41. Glennie MJ, French RR, Cragg MS, Taylor RP. Mechanisms of killing by anti-CD20 monoclonal antibodies. *Mol Immunol.* 2007;44(16):3823-3837.
42. Cragg MS, Morgan SM, Chan HT, et al. Complement-mediated lysis by anti-CD20 mAb correlates with segregation into lipid rafts. *Blood.* 2003; 101(3):1045-1052.
43. Cardarelli PM, Quinn M, Buckman D, et al. Binding to CD20 by anti-B1 antibody or F(ab′)(2) is sufficient for induction of apoptosis in B-cell lines. *Cancer Immunol Immunother.* 2002;51(1):15-24.
44. Beers SA, Chan CH, James S, et al. Type II (tositumomab) anti-CD20 monoclonal antibody out performs type I (rituximab-like) reagents in B-cell depletion regardless of complement activation. *Blood.* 2008;112(10):4170-4177.
45. Zhuang S, Schnellmann RG. A death-promoting role for extracellular signal-regulated kinase. *J Pharmacol Exp Ther.* 2006;319(3):991-997.
46. Ivanov A, Krysov S, Cragg MS, Illidge T. Radiation therapy with tositumomab (B1) anti-CD20 monoclonal antibody initiates extracellular signal-regulated kinase/mitogen-activated protein kinase-dependent cell death that overcomes resistance to apoptosis. *Clin Cancer Res.* 2008;14(15): 4925-4934.
47. di Mari JF, Davis R, Safirstein RL. MAPK activation determines renal epithelial cell survival during oxidative injury. *Am J Physiol.* 1999;277(2 pt 2):F195-F203.
48. Kansas GS, Tedder TF. Transmembrane signals generated through MHC class II, CD19, CD20, CD39, and CD40 antigens induce LFA-1-dependent and independent adhesion in human B cells through a tyrosine kinase-dependent pathway. *J Immunol.* 1991;147(12):4094-4102.
49. Ivanov A, Beers SA, Walshe CA, et al. Monoclonal antibodies directed to CD20 and HLA-DR can elicit homotypic adhesion followed by lysosome-mediated cell death in human lymphoma and leukemia cells. *J Clin Invest.* 2009;119(8):2143-2159.
50. Xie L, Qiao X, Wu Y, Tang J. β-Arrestin1 mediates the endocytosis and functions of macrophage migration inhibitory factor. *PLoS One.* 2011;6(1): e16428.